CHEMBIOCHEM

Supporting Information

Engineering an Allosteric Binding Site for Aminoglycosides into TEM1-β-Lactamase

Alexander N. Volkov,[a, d] Humberto Barrios,[a] Pascale Mathonet,[a] Christine Evrard,[b] Marcellus Ubbink,[c] Jean-Paul Declercq,[b] Patrice Soumillion,*[a] and Jacques Fastrez*[a]

cbic_201000568_sm_miscellaneous_information.pdf

Supplementary material

Isotermal titration calorimetry data

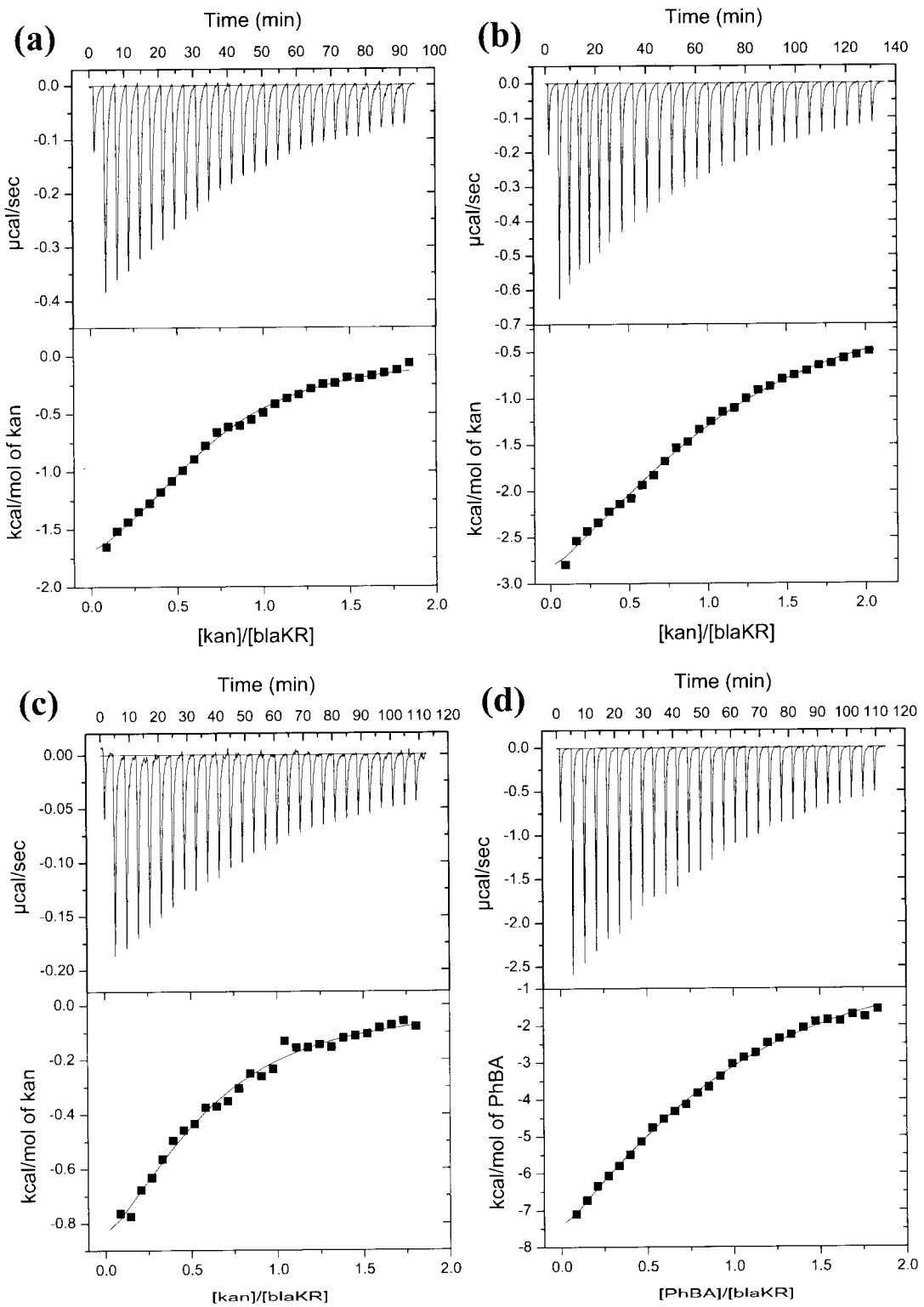

Figure S1. Representative ITC curves for the binding of (a) kan to blaKR in MES, (b) kan to blaKR in sodium cacodylate, (c) kan to blaKR-PhBA in MES, and (d) PhBA to blaKR in MES. The top and bottom panels show, respectively, the raw data after the baseline correction and the integrated data corrected for the heat of dilution of the ligand. The solid lines in the bottom panels are the best fits to the 1:1 binding model. The experiments were performed in 20 mM corresponding buffer, pH 6.6, at 303 K, with the concentrations of (a) - (b) 0.11 mM blaKR and 1 mM kan; (c) 0.12 mM blaKR, 2.82 mM PhBA, and 1 mM kan; and (d) 0.14 mM blaKR and 1.19 mM PhBA.

X-Ray crystallography. The data were processed by XDS and XSCALE (S1). The structure of Bla-KR was solved by molecular replacement with Phaser (S2) using as model the structure of *E.coli* TEM1 β-lactamase [PDB code 1BTL (S3)]. The model was corrected and completed using Arp-Warp (S4). Some minor manual adjustments were performed using O (S5) or Coot (S6). The structure was refined with Refmac5 (S7) of the CCP4 suite (S8). The solvent molecules were positioned using Arp-Warp (S4). In one position, a much heavier atom than a water molecule had to be accommodated, and it was interpreted as a Zn^{2+} ion. This ion is neighboring N^{δ} atoms of His_{133} and His_{138} and $O^{\varepsilon 1}$ of Glu_{90}, belonging to a symmetry-related molecule and a water molecule. Surprisingly, the structure of Bla-KR.SO_4 was not isomorphous and could not be refined immediately, even starting with rigid-body refinement at low resolution. The structure of Bla-KR was thus used as a model for molecular replacement using Phaser (S2). During the refinement, it appeared that the Zn^{2+} ion was also conserved and that two sulphate ions had to be positioned. On the other hand, no electron density suitable for a molecule of kanamycin could be observed. The final coordinates and structure factors were deposited in the Protein Data Bank [PDB ID 2V1Z (Bla-KR) and 2V20 (Bla-KR.SO_4)]. Refinement statistics are presented in Table S2.

NMR Spectroscopy. All NMR data were processed with Azara 2.7 (provided by W. Boucher and Department of Biochemistry, University of Cambridge; available from http://www.bio.cam.ac.uk/azara/) and analyzed in Ansig for Windows (S9). Backbone amide resonance assignments were derived manually from a suit of TROSY-type 3D experiments (S10, S11): HNCA, HN(CO)CA, CBCA(CO)NH, and HNCO for both free and PhBA-bound BlaKr and an additional HNCACB for the free protein.

NMR chemical shift titration curves (Figure S1) were analyzed with a two-parameter non-linear least-squares fit using a one-site binding model corrected for the dilution effect (equations S1-S2):

$$\Delta\delta_{binding} = \frac{1}{2}\Delta\delta_0 \left(A - \sqrt{A^2 - 4R}\right) \qquad \text{(S1)}$$

$$A = 1 + R + \frac{[KanA]_0 + R[BlaKr]_0}{[KanA]_0[BlaKr]_0 K_B} \qquad \text{(S2)}$$

where $\Delta\delta_{binding}$ is the chemical shift perturbation at a given protein ratio, $\Delta\delta_0$ is the chemical shift perturbation at 100 % KanA bound, R is the [KanA]/[BlaKr] ratio at a given point, $[KanA]_o$ and $[BlaKr]_o$ are the concentrations of KanA stock solution used for the titration and the starting BlaKr solution, respectively, and K_B is the binding constant of the complex. Thus, $\Delta\delta_{binding}$ and R are the dependent and independent variables, respectively, and $\Delta\delta_0$ and K_B are the fitted parameters.

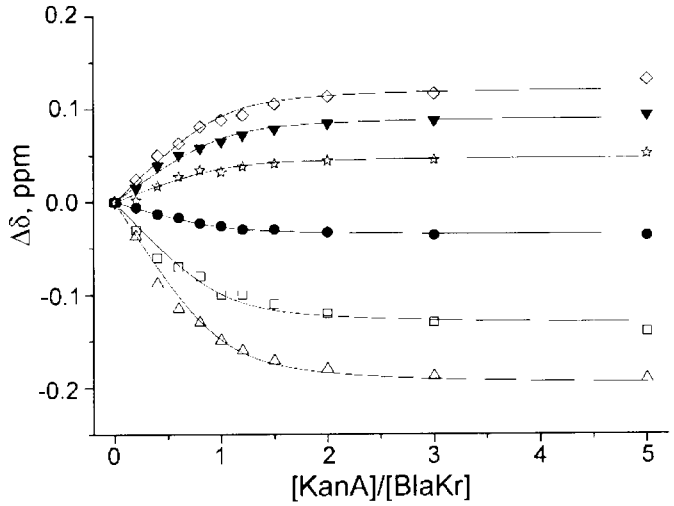

Fig. S2. NMR titration of ^{15}N BlaKr with KanA. The solid lines represent the best fit to a 1:1 binding model with the shared K_d of 32 ± 5 μM. Chemical shift perturbations of backbone amide ^{1}HN (filled symbols) and ^{15}N atoms (open symbols) are shown for the BlaKr residues R_{41a} (squares), S_{243} (triangles), G_{267} (inverted triangles), S_{268} (diamonds), R_{269} (circles), and Q_{278} (stars). For clarity, the titration profile of R_{41a} ^{1}HN, included in the global fit but overlapping heavily with that of R_{269} ^{1}HN, is not shown. The experimental errors are comparable to the symbol size.

Table S1. Relationship between parameters determined as a function of [aminoglycoside] at constant [aminosulfonate]=[I] (parameters of scheme in Fig. 2*D*). [a] ND = not determined (see Supplementary Methods below).

Plot	Observed	Derived
k_{cat}	$k^{0}_{cat,app}$	k^{0}_{cat}
	$k^{A}_{cat,app}$	k^{A}_{cat}
	$K_{d,app}$	ND [a]
K_m	$K^{0}_{m,app}$	$K^{0}_{m}\left(1+\frac{[I]}{K^{0}_{I}}\right)$
	$K^{A}_{m,app}$	$K^{A}_{m}\left(1+\frac{[I]}{K^{A}_{I}}\right)$
	$K_{d,app}$	$K_{d,ES}$
k_{cat}/K_m	$\left(\frac{k^{0}_{cat}}{K^{0}_{m}}\right)_{app}$	$\frac{k^{0}_{cat}}{\left[K^{0}_{m}\left(1+\frac{[I]}{K^{0}_{I}}\right)\right]}$
	$\left(\frac{k^{A}_{cat}}{K^{A}_{m}}\right)_{app}$	$\frac{k^{A}_{cat}}{\left[K^{A}_{m}\left(1+\frac{[I]}{K^{A}_{I}}\right)\right]}$
	$K_{d,app}$	$\frac{K_{d,E}\left(1+\frac{[I]}{K^{0}_{I}}\right)}{1+\frac{[I]}{K^{A}_{I}}}$

Table S2. Data collection, processing and refinement statistics of BlaKr X-ray structures.

		BlaKr	BlaKr.SO_4
Data collection and processing			
Space group		$P2_12_12_1$	$P2_12_12_1$
Unit cell	a (Å)	47.11(1)	46.08(3)
	b (Å)	70.61(3)	72.14(5)
	c (Å)	78.31(3)	73.50(4)
X-ray source		ESRF	EMBL c/o DESY
Synchrotron beam line		BM30A	X12
Detector type		MarCCD 165	MarCCD 225
Wavelength (Å)		0.97976	0.92021
Resolution (Å)	overall (ov)	40.37 – 1.60	18.00 – 1.67
	highest shell (hs)	1.65 – 1.60	1.75 – 1.67
Measured reflexions		120750	101477
Unique reflexions		34091	28557
Completeness (%) ov/hs		96.7/93.2	98.0/92.3
Rsym ov/hs		0.038/0.220	0.045/0.253
$<I/\sigma(I)>$ ov/hs		23.9/8.2	18.0/4.5
Refinement			
Rfactor		0.1689	0.1798
Rfree		0.2061	0.2232
Estimated overall coordinate error (Å)			
based on Rfree		0.093	0.113
based on Max. likelihood		0.053	0.076
Limits (residue numbers) of observed electron density		1-270	1-269
R.M.S. deviation from ideality:	bond lengths (Å)	0.018	0.020
	bond angles (°)	1.67	1.83
Nr of solvent molecules		352	274
of Zn^{2+} ions		1	1
of SO_4^{2-} ions		-	2
Mean B values (Å^2)	Main chain	17.5	16.8
	Side chains	20.4	19.3
	Solvent	32.4	32.6
Ramachandran: % in	favoured regions	98.5	98.1
	allowed regions	100	100

Table S3: Correspondence between residues numbering assigned in the X-ray structures 2v1z and 2v20 and Ambler numbering

1	P27	48	M68	95	D115	142	L162	189	D209	236	S258
2	E28	49	M69	96	G116	143	D163	190	W210	237	R259
3	T29	50	S70	97	M117	144	R164	191	M211	238	I260
4	L30	51	T71	98	T118	145	W165	192	E212	239	V261
5	V31	52	F72	99	V119	146	E166	193	A213	240	V262
6	K32	53	K73	100	R120	147	P167	194	D214	241	I263
7	V33	54	V74	101	E121	148	E168	195	K215	242	Y264
8	K34	55	L75	102	L122	149	L169	196	V216	243	T265
9	D35	56	L76	103	C123	150	N170	197	A217	244	T266
10	A36	57	C77	104	S124	151	E171	198	G218	245	G267
11	E37	58	G78	105	A125	152	A172	199	P219	246	S268
12	D38	59	A79	106	A126	153	I173	200	L220	247	R269
13	Q39	60	V80	107	I127	154	P174	201	L221	248	K270
14	L40	61	L81	108	T128	155	N175	202	R222	249	K271
15	C41	62	S82	109	M129	156	D176	203	S223	250	T272
16	R41a	63	R83	110	S130	157	E177	204	A224	251	D273
17	T41b	64	I84	111	D131	158	R178	205	L225	252	E274
18	S41c	65	D85	112	N132	159	D179	206	P226	253	R275
19	H41d	66	A86	113	T133	160	T180	207	A227	254	N276
20	R41e	67	G77	114	A134	161	T181	208	G228	255	R277
21	P41f	68	Q88	115	A135	162	M182	209	W229	256	Q278
22	C42	69	E89	116	N136	163	P183	210	F230	257	I279
23	R43	70	Q90	117	L137	164	V184	211	I231	258	A280
24	V44	71	L91	118	L138	165	A185	212	A232	259	E281
25	G45	72	G92	119	L139	166	M186	213	D233	260	I282
26	Y46	73	R93	120	T140	167	A187	214	K234	261	G283
27	I47	74	R94	121	T141	168	T188	215	S235	262	A284
28	E48	75	I95	122	I142	169	T189	216	G236	263	S285
29	L49	76	H96	123	G143	170	L190	217	A237	264	L286
30	D50	77	Y97	124	G144	171	R191	218	G238	265	I287
31	L51	78	S98	125	P145	172	K192	219	R240	266	K288
32	N52	79	Q99	126	K146	173	L193	220	R241	267	H289
33	S53	80	N100	127	E147	174	L194	221	G242	268	W290
34	G54	81	D101	128	L148	175	T195	222	S243		
35	K55	82	L102	129	T149	176	G196	223	R244		
36	I56	83	V103	130	A150	177	E197	224	G245		
37	L57	84	K104	131	F151	178	L198	225	I246		
38	E58	85	Y105	132	L152	179	L199	226	I247		
39	S59	86	S106	133	H153	180	T200	227	A248		
40	F60	87	P107	134	N154	181	L201	228	A249		
41	R61	88	V108	135	M155	182	A202	229	L250		
42	P62	89	T109	136	G156	183	S203	230	G251		
43	E63	90	E110	137	D157	184	R204	231	P252		
44	E64	91	K111	138	H158	185	Q205	232	D254		
45	R65	92	H112	139	V159	186	Q206	233	G255		
46	F66	93	L113	140	T160	187	L207	234	K256		
47	P67	94	T114	141	R161	188	I208	235	P257		

References

S1. W. Kabsch, *J. Appl. Crystallogr.* **1993**, *26*, 795-800.

S2. McCoy, A.J.; Grosse-Kunstleve, R.W.; Storoni, L.C.; Read, R.J. *Acta Crystallogr. sect.* **2005**, *D 61*, 458.

S3. Jelsch, C.; Mourey, L.; Masson, J.M.; Samama, J.P. *Proteins* **1993**, *16*, 364.

S4. Morris, R.J.; Perrakis, A; Lamzin, V.S. *Methods Enymol.* **2003**, *374*, 229.

S5. Jones, T.A.; Zou, J.-Y.; Cowan, S.W.; Kjeldgaard, M. *Acta Crystallogr. sect. A*, **1991**, *47*, 110.

S6. Emsley, P.; Cowtan, K. *Acta Crystallogr. sect. D* **1994**, *60*, 2126.

S7. Murshudov, G. N.; Vagin, A. A.; Dodson, E .J. *Acta. Crystallogr. sect. D* **1997**, *53*, 240.

S8. Collaborative Computational Project, Number 4. *Acta Crystallogr. sect.* **1994**, *D 50*, 760.

S9. Helgstrand, M.; Kraulis, P.J.; Allard, P.; Hard, T. *J. Biol. NMR* **2000**, *18*, 329.

S10. Salzmann, M.; Pervushin, K.; Wider, G.; Senn, H.; Wüthrich, K. *Proc. Natl. Acad. Sci. USA.* **1998**, *95*, 13585.

S11. Salzmann, M.; Wider, G.; Pervushin, K.; Senn, H.; Wüthrich, K. *J. Am. Chem. Soc.* **1999**, *121*, 844.